

Extended Far–Infrared CO Emission in the Orion OMC–1 Core¹

María J. Sempere², José Cernicharo, Bertrand Lefloch³, Eduardo González–Alfonso⁴
 CSIC, IEM, Dpto. Física Molecular, Serrano 121, E–28006 Madrid, Spain.

Sarah Leeks

Physics Department, Queen Mary & Westfield College, University of London, Mile End
 Road, London E1 4NS, UK

ABSTRACT

We report on sensitive far–infrared observations of ¹²CO pure rotational transitions in the OMC–1 core of Orion. The lines were observed with the Long Wavelength Spectrometer (LWS) in the grating mode on board the Infrared Space Observatory (ISO), covering the 43–197 μm wavelength range. The transitions from $J_{up} = 14$ up to $J_{up} = 19$ have been identified across the whole OMC–1 core and lines up to $J_{up} = 43$ have been detected towards the central region, KL/IRc2. In addition, we have taken high–quality spectra in the Fabry–Perot mode of some of the CO lines. In KL/IRc2 the lines are satisfactorily accounted for by a three–temperature model describing the plateau and ridge emission. The fluxes detected in the high– J transitions ($J_{up} > 34$) reveal the presence of a very hot and dense gas component ($T = 1500 - 2500$ K; $N(\text{CO}) = 2 \times 10^{17} \text{ cm}^{-2}$), probably originating from some of the embedded sources previously observed in the H₂ near–infrared lines. At all other positions in the OMC–1 core, we estimate kinetic temperatures ≥ 80 K and as high as 150 K at some positions around IRc2, from a simple Large–Velocity Gradient model.

Subject headings: infrared: ISM: lines and bands–ISM: molecules–line: identification– molecular data–radiative transfer– ISM: individual (OMC–1)

¹ Based on observations with ISO, an ESA project with instruments funded by ESA Member States (especially the PI countries: France, Germany, the Netherlands and the United Kingdom) and with participation of ISAS and NASA.

²sempere@astro.iem.csic.es

³Now at Observatoire de Grenoble, BP 53, F–38041 Grenoble, CÉDEX 9, France. lefloch@obs.ujf-grenoble.fr

⁴Also at the Universidad de Alcalá de Henares, Departamento de Física, Campus Universitario, E–28871 Alcalá de Henares, Madrid, Spain.

1. Introduction

The Orion molecular cloud is the prime example of high-mass star forming regions and due to its proximity one of the most extensively studied sources. The numerous observations performed in the millimeter and submillimeter range (see Blake et al. 1987 and Genzel & Stutzki 1989 for a review) have shown that the emission arises from three main components. The bulk of the molecular gas in the extended *ridge* (typical densities $\leq 10^4 \text{ cm}^{-3}$) is heated up to 50–60 K by the UV field of the Trapezium stars. The molecular emission near the high-velocity outflow, the *plateau*, is distributed in a highly anisotropic region of $40''$ in size with a mean density $\leq 10^6 \text{ cm}^{-3}$. The plateau consists of gas heated to temperatures of 80–150 K distributed in a low-velocity component centered on IRc2 and in a bipolar high-velocity component orthogonal to the latter. Finally, the *hot core* ($T = 400 - 500 \text{ K}$) of IRc2 is a compact source ($10''$) with densities up to 10^7 cm^{-3} . Its high-excitation molecular emission probably arises from material shocked by the interaction of the high-velocity outflow with the ambient gas.

The OMC-1 core has been widely studied in various molecular tracers. Among these, CO is of great interest because observations at different transitions delimit regions with marked contrasts in their physical characteristics. Most are low- J ($J_{up} \leq 4$) observations that trace the extended low/moderate density gas, and the bulk of the outflow gas. Higher- J transitions ($J_{up} \geq 6$) are sensitive to the denser and higher-temperature gas of the plateau or the hot core, however they are much less sensitive to those values from the ridge. Multiple CO line observations towards IRc2 carried out with the KAO in the submillimeter/far-infrared range (see e.g. Boreiko et al. 1989) suggest evidence for a hot gas component at 600–750 K in the high-velocity and (possibly) low-velocity plateau, based on the few flux measurements at $J_{up} > 22$. However, the large uncertainties in the atmospheric transmission yield considerable variations in the parameters of this hot gas component. The ISO satellite offered us the possibility of assessing in a more systematic and comprehensive way the temperature distribution in Orion. We present in this Letter the first large-scale survey of the far-infrared CO lines in the Orion OMC-1 core.

2. Observations and Results

Five LWS-grating rasters were performed in the LWS01 mode (range 43–197 μm) with a spectral resolution of 0.3–0.6 μm ($R = \lambda/\Delta\lambda \sim 150 - 300$). A total of 23 positions (6 scans per position) with an angular separation of $90''$ (\sim beam size) were observed around IRc2. The central position was included in each raster in order to check the relative calibration of the observations. The uncertainties in the absolute calibration are estimated to be $\sim 30\%$.

After pre-reduction (pipeline 7) the data were reprocessed in order to remove non-linear effects (Leeks et al. 1999). The size of the LWS beam is actually close to $70''$ (E. Caux, priv. comm.).

The spectra observed at each position (36 scans for the central one) were averaged together in order to minimize the noise level. The statistical errors of the measured lines fluxes are negligible. The transitions at $\lambda < 90 \mu\text{m}$ are effected by additional uncertainties in the determination of the continuum level (hence the baseline subtraction), as well contamination from neighboring lines. The confusion level is $\sim 3 \times 10^{-18} \text{ W cm}^{-2}$ in the averaged spectra. However, we checked that all the features identified in the averaged spectra were present in all of the original scans. Figure 1 shows the LWS spectra in the range $135\text{--}190 \mu\text{m}$ for the positions where the CO lines could be unambiguously identified. Besides CII ($158 \mu\text{m}$) and OI ($63 \mu\text{m}$ and $146 \mu\text{m}$) fine-structure atomic lines, the CO emission, together with that of H_2O , dominates the OMC-1 far-infrared spectrum. Among the molecular species detected in Orion at infrared wavelengths, CO appears to be the most widespread (a full description of the IRc2 spectrum can be found in Cernicharo et al. 1999a, 1999b, hereafter C99a, C99b). At all of the positions, we observe the pure rotational transitions from $J_{up}=14$ to $J_{up}=19$, but only the lines up to $J_{up}=17$ have a SNR high enough to allow confident detection outside IRc2. At large angular distances from the central region ($> 180''$), the CO lines become very weak and the spectra are dominated by the atomic fine-structure lines. The CO integrated fluxes at fifteen selected positions are given in Table 1. Some of lines are contaminated by nearby features (OI at $145.6 \mu\text{m}$, OH at $163.2 \mu\text{m}$ and H_2O at different wavelengths), whose contributions have been estimated from complementary Fabry-Perot observations (C99a) or from the grating data where the line separation was about $0.3 \mu\text{m}$.

Towards the central region, the consecutive pure rotational lines from $J_{up}=14$ up to $J_{up}=43$ could be identified. Due to the presence of numerous unresolved components, the calibration of the high- J transitions ($J_{up} \geq 34$) is somewhat uncertain. When observing the H_2O lines towards IRc2 at high spectral resolution with the LWS in the Fabry-Perot mode ($R \sim 7000$), several CO transitions, between $J_{up}=14$ and $J_{up}=33$, were also detected in some detector bands (Fig. 2; for details on the observations, see C99a). The Fabry-Perot (hereafter FP) fluxes agree to better than 30% with the grating data, except for the $J_{up}=16$ and the $J_{up}=28$ lines where the differences reach 50%. In view of the possible uncertainties in the actual pipeline, we have used the grating fluxes for these two lines. Quite remarkably, the line intensities are nearly constant from $J_{up}=18$ up to $J_{up}=21$ indicating that the lines are optically thick and that the emitting regions are similar in size. The line intensity merely decreases by a factor of three for the following transitions up to $J_{up}=28$. All of the lines have typical widths of $\Delta v \simeq 60 \text{ km s}^{-1}$ (HPFW), i.e. they are partially resolved by the

FP.

3. Discussion

3.1. The Ridge

In order to determine the temperature of the gas traced by the CO lines detected in the OMC–1 core, we have modeled the emission of a gas layer with a column density of $N(\text{CO}) = 10^{19} \text{ cm}^{-2}$ for various densities, $n(\text{H}_2)$, and temperatures. The CO fluxes were computed using a simple Large–Velocity Gradient approach. For the LWS wavelength range the dust opacity is still low enough that the coupling between dust and gas can be neglected. The adopted linewidth in the model is $\Delta v = 10 \text{ km s}^{-1}$ for positions close to the center ($\pm 90''$, $\pm 90''$) and $\Delta v = 5 \text{ km s}^{-1}$ for the points more distant from IRc2.

We display in Fig. 3 b–d the expected fluxes for the transitions $J_{up} \leq 25$ with $n(\text{H}_2)$ densities in the range $4 - 40 \times 10^4 \text{ cm}^{-3}$ for specific temperatures. The temperatures shown are those which give the best match to the fluxes measured at three typical positions in the core: halfway between the bar and the main core ($90''$, $-90''$); south of IRc2 towards the S6 protostellar source ($0''$, $-90''$); the extended ridge ($0''$, $-180''$). For densities in the range $4 - 40 \times 10^4 \text{ cm}^{-3}$, typical of those measured in the OMC–1, temperatures larger than 80 K are required to account for *all* of the observed fluxes. Lower temperatures of $\sim 60 \text{ K}$ fail to reproduce the observations by a factor of two or more (see Fig. 3). Around the central position, ($\pm 90''$, $\pm 90''$), we find evidence for warm gas with $T \geq 120 \text{ K}$ and densities of the order of $\sim 10^5 \text{ cm}^{-3}$. The column density adopted in our model appears as an upper limit since it was observed towards the IRc2 core (Blake et al. 1987). If we adopt a lower column density of $5 \times 10^{18} \text{ cm}^{-2}$ for positions remote from IRc2, in closer agreement with CO observations at millimeter wavelengths (Bally et al. 1987), reasonable fits are obtained by increasing the kinetic temperature by 10–20%, or conversely increasing the density by a factor of 2–3. This does not effect our conclusions about the extended warm component around the hot core. From Fig. 3, it appears that low– J observations bring very little constraints to the temperature determinations in our modeling. The kinetic temperatures derived from KAO observations of the $J_{up} = 7$ line ($\sim 90 - 100 \text{ K}$) at $100''$ resolution by Schmid–Burgk et al. (1989) agree reasonably well for the S6 region and close to IRc2.

On the western side of the ridge, our modeling requires temperatures above 100 K or more, and/or high column densities and volume densities to account for the observed fluxes (see Table 1). The KAO data suggest moderate temperatures around $\sim 50 \text{ K}$, although it is difficult to compare both sets of data due to the larger beam and coarse sampling of

the former. We note that some contamination in our data from the IRc2 region within a possible LWS error beam cannot be excluded and could reduce the derived column densities and/or kinetic temperatures. Also the LWS beam profile is known to be rotationally asymmetric for an extended source and could account for some of the discrepancies.

3.2. The Orion–KL/IRc2 Region

The emission in the far-infrared CO lines from $J_{up}=18$ to 33 can be reasonably explained by a simple two-temperatures model of the plateau region. First we note that a single temperature model cannot reproduce both the flux of the high ($J_{up} > 28$) and low- J lines. On the other hand, the range of temperatures reported in the extended ridge imply that its contribution becomes negligible with respect to the plateau (see also Fig. 3 and below) for transitions above $J_{up} = 18$. The physical properties of the gas in the different regions (in particular the plateau) were chosen as close as possible to those of Blake et al. (1987). The low-velocity plateau is modeled as a two-shell region expanding at 25 km s^{-1} with a micro-turbulent velocity of 10 km s^{-1} . The line fluxes were calculated with the radiative transfer code developed by Gonzalez-Alfonso & Cernicharo (1997) and were convolved with the expected instrumental profile (see Fig. 2) which accounts for the FP instrumental response (E. Caux, priv. comm.). We have adopted standard properties for the dust (silicate) grains: a typical radius of $0.1 \mu\text{m}$ and a standard gas-to-dust mass ratio of 100. The inner region gives rise to the entire emission of the $J_{up} = 33$ and $J_{up} = 28$ lines, to the bulk of the emission of the $J_{up} = 24$ line and to a significant contribution of the lower- J lines. The colder gas of the plateau also contributes to the emission of the low- J lines. Based on our study of the H_2O emission in Orion by Cernicharo et al. (C99a), we assume that the density is high enough to almost thermalize the CO lines: $\sim 10^7 \text{ cm}^{-3}$ for the inner region and $\sim 10^6 \text{ cm}^{-3}$ for the external one, close to the estimates derived by Blake et al. (1987). We use the standard CO abundance of 1.2×10^{-4} . The ratio of the $J_{up} = 33$ to the $J_{up} = 28$ lines sets an upper limit of $\sim 500 \text{ K}$ to the temperature of the inner region: a higher value would imply a lower contrast between the two lines for any CO column density. For a lower temperature ($\sim 350 \text{ K}$), the high column density needed to account for the $J_{up} = 33$ line would then overestimate the ^{13}CO lines, whereas they are hardly detected (we adopt an upper limit of 3000 Jy). We have adopted a temperature $T = 400 \text{ K}$ for the inner plateau region. The resulting column density is $N(\text{CO}) = 10^{19} \text{ cm}^{-2}$; the outer and inner radii are $3 \times 10^{16} \text{ cm}$ ($4.5''$) and $2.2 \times 10^{16} \text{ cm}$ respectively. For the external shell (outer radius = $7 \times 10^{16} \text{ cm}$), the temperature is $T = 300 \text{ K}$ and the column density $N(\text{CO}) = 3.5 \times 10^{18} \text{ cm}^{-2}$. The assumed column densities agree with the values quoted in the literature (Blake et al. 1987).

The agreement with the line profiles is very satisfying taking into account the simple hypothesis used. The apparent high-velocity emission is fully reproduced by convolving with the broad-wing instrumental response (Fig. 2). Down to the sensitivity of these observations, we do not detect in this wavelength range any emission from the very high-velocity gas around IRc2. Comparison with all the lines observed by the LWS (either in FP or grating mode) proves to be satisfying up the $J_{up} = 33$ transition. We have added to our modeling the contribution of the extended ridge, as a layer at $T = 80$ K (see Sect. 3.3) with a column density of $N(\text{CO}) = 4 \times 10^{19} \text{ cm}^{-2}$. The resulting fit and the contributions of the different regions are shown in Fig. 3. As a whole, the emission observed towards the IRc2 core can be satisfactorily accounted for by two regions of the plateau gas at different temperatures: ~ 300 K and ~ 400 K, and from the ridge contributing significantly up to the $J_{up} = 16$ line. Note that since the central part of the line profiles is only partially resolved by the FP, we cannot exclude that a part of the warm component modeled actually arises from the hot core (where $\Delta v \approx 5 \text{ km s}^{-1}$). Therefore, the emission from the $T = 400$ K component should be considered as the combined emission of the plateau and the hot core. The contribution of the ridge seems to be underestimated in our model. However, as for the adjacent positions, the contribution from an error beam could effect the observed fluxes.

3.3. The High- J CO lines

The higher- J transitions ($J_{up} > 34$) observed with the grating mode are largely contaminated by other emission lines. Using our FP data we have estimated the contribution of the strongest adjacent lines (OH, H₂O and NH₃) to the CO fluxes. In view of the high density of spectral lines for $\lambda < 90 \mu\text{m}$, additional contamination by other weaker lines cannot be discarded (C99a,b). We note, however, that the lines are well above the confusion level and that most of the observed flux must arise from CO itself.

After correction, all the CO lines observed either in FP or grating mode lay above the model of the plateau and the ridge (Fig. 3a), showing evidence for a hotter gas component. In the absence of other information on the spatial location and the kinematics of this gas, we speculate that such emission arises from the shocked regions of interaction of the Orion outflows with the ambient medium, detected in the $2.12 \mu\text{m}$ lines. All sources of strong H₂ emission (BN, KL, PK1, PK2; Beckwith et al. 1983) are located within our $70''$ beam. We modeled the high- J CO emission using a Large-Velocity Gradient (LVG) approach with parameters representative of the H₂ Peak 1 region: a size of $10''$, a density $n(\text{H}_2) \sim 3 \times 10^7 \text{ cm}^{-3}$ for the shocked emitting region, and a linewidth $\Delta v = 30 \text{ km s}^{-1}$. The fluxes are roughly accounted for by a gas layer at $T \sim 1500 - 2000$ K and a column

density $N(\text{CO}) \sim 6 \times 10^{17} \text{ cm}^{-2}$, implying a shell thickness of $1.6 \times 10^{14} \text{ cm}$. These values are merely indicative due to the lack of spectral and spatial information, but are consistent with those predicted by shock models (e.g., Flower & Pineau des Forêts, 1999).

Acknowledgements.

This work has been partially supported by the Spanish DGES under grant PB96–0883 and by PNIE grant ESP97–1618–E. SJL acknowledges receipt of a PPARC award. We thank Drs S. Pérez–Martínez and J.R Goicoechea for their help in the data reduction and Dr. E. Caux for providing us with the Fabry–Perot instrumental profile.

REFERENCES

- Bally, J., Stark, A.A., Wilson, R.W., & Langer, W.D. 1987, ApJ, 312, L45.
- Blake, G.A., Sutton, E.C., Masson, C.R., & Phillips, T.G. 1987, ApJ, 315, 621.
- Beckwith, S., Evans, N.J., II, Gatley, I., Gull, G., & Rusell, R. W. 1983, ApJ, 264, 152.
- Boreiko, R.T., Betz, A.L., & Zmuidzinas, J. 1989, ApJ, 337, 332.
- Boreiko, R.T., & Betz, A.L. 1989, ApJ, 346, L97.
- Cernicharo, J., et al. 1999, in The Universe as seen by ISO, ESA-SP427 (Noordwijk: ESA), 565. (C99a)
- Cernicharo, J., et al. 1999, in The Universe as seen by ISO, ESA-SP427(Noordwijk: ESA), 651. (C99b)
- Genzel, R., & Stutzki, J. 1989, ARA&A, 27, 41.
- González–Alfonso, E., & Cernicharo, J. 1997, A&A, 322, 938.
- Graf, U.U., Genzel, R., Harris, A.I., Hills, R.E., Rusell, A.P.G., & Stutzki, J. 1990, ApJ, 358, L49.
- Howe, J.E., Jaffe, D.T., Grossman, E.N., Wall, W.F., Mangum, J.G., & Stacey, G.J. 1993, ApJ, 410, 179.
- Flower, D.R., & Pineau des Forêts, G. 1999, MNRAS, 308, 271.
- Leeks, S.J., Swinyard, B.M., Lim, T.L., & Clegg, P.E. 1999, in The Universe as seen by ISO, ESA-SP427(Noordwijk: ESA), 81.

Schmid-Burgk, J., Densing, R., Krügel, E., et al. 1989, A&A, 215, 150.

Schultz, A. J., Krügel, E., & Beckmann, U. 1992, A&A, 264, 629.

Watson, D.M., Genzel, R., Townes, C.H., & Storey, J.W.V. 1985, ApJ, 298, 316.

Transition	14-13	15-14	16-15	17-16	
E_{up} (K)	581	664	752	846	
λ (μm)	185.9	173.6	162.8	153.2	
Position	Flux(10^{-18} W cm^{-2})				T(K)
(0'', -270'')	4.9	4.6	1.7	0.22	–
(0'', -180'')	7.5	10	6.5	2.2	80
(0'', -90'')	43.	42.	40	3.2	120
(0'', 90'')	32	48	38	4.	120
(0'', 180'')	2.8	4.5	2.7	1.3	80
(-270'', 0'')	0.8	2.2	0.33	0.3	–
(-180'', 0'')	1.9	1.3	0.13	–	60
(-90'', 0'')*	16	17	19	1.9	120
(90'', 0'')	16	18	15	3.9	100
(180'', 0'')	7.1	7.0	4.5	2.3	80
(270'', 0'')	2.7	3.0	0.64	–	–
(-90'', 90'')*	16	23	25	6.2	100
(90'', -90'')	18	19	25	3.8	120
(90'', 90'')	17	18	6.7	2.5	80
(-90'', -90'')*	19	29	27	–	100

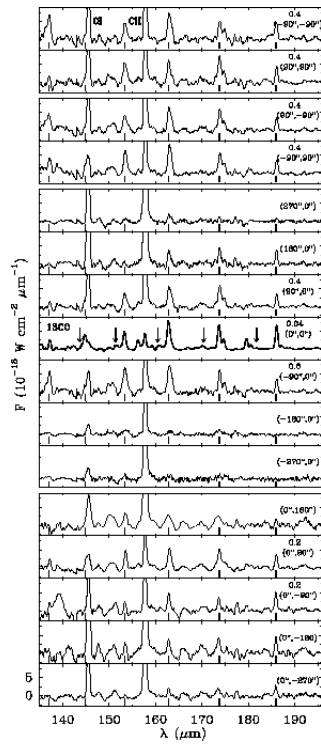
Table 1 : CO line fluxes measured in the extended ridge of OMC–1.

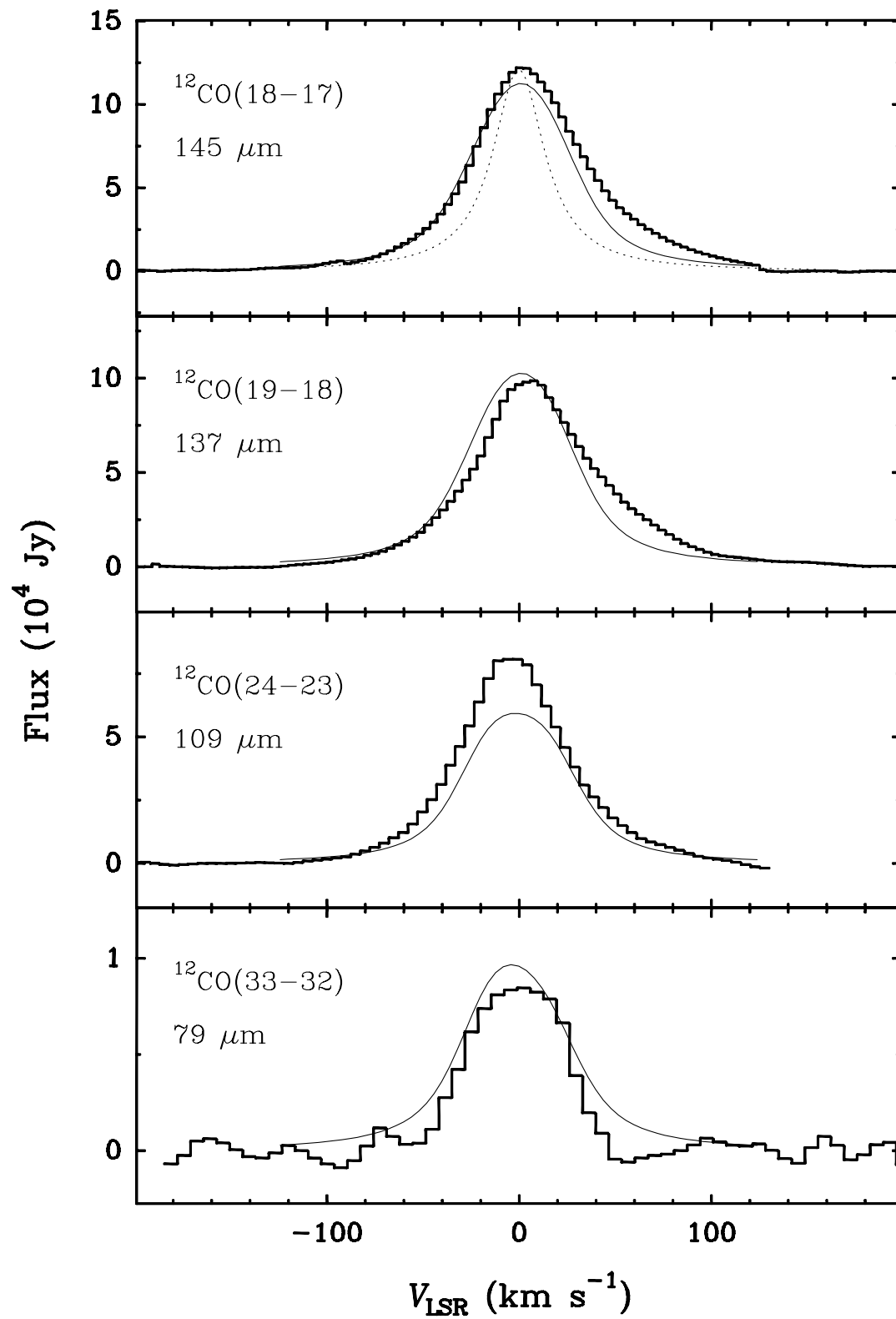
The positions for which the line fluxes could be contaminated by emission from IRc2 within the LWS error beam are marked with an asterisk (see text).

Fig. 1.— LWS grating spectra from the observed positions around IRc2 between 135–197 μm . Lower marks indicate the ^{12}CO rotational transitions from $J_{up} = 14$ to $J_{up} = 19$. At the central position ^{13}CO transitions are marked by the arrows. Some spectra have been multiplied by a scale factor indicated at the top right of each panel.

Fig. 2.— A montage of select CO transitions observed towards IRc2 with the LWS in the Fabry-Perot mode (thick line). We have indicated (thin line) the modeled emission of the plateau (see text). The instrumental response of the Fabry-Perot at 145 μm is indicated on the $J_{up} = 18$ spectra (dotted line).

Fig. 3.— **a)** Integrated flux of the CO lines detected towards the IRc2 region. The modeled contributions from the plateau (P, thin line) and the ridge (R, dotted thin) are shown. A hot gas component (HG) was introduced (dashed line) to reproduce the emission at $J_{up} > 34$. The arrows mark the fluxes of the observed CO lines possibly overestimated due to contamination by weak adjacent lines. We have superposed (empty squares) the values estimated for the ISO beam size from previous work: $J_{up}= 4$ (Schultz et al., 1992); 6 (Graf et al., 1990); 7 (Schmid-Burgk et al. 1989; Howe et al. 1993); 21 (Boreiko & Betz, 1989); 22-34 (Watson et al 1985). **b,c,d)** Expected fluxes for the CO lines up to $J_{up} = 25$ observed in the extended ridge with the ISO LWS beam, for kinetic temperatures comprised between 60–120 K, H_2 densities $4 - 40 \times 10^4 \text{ cm}^{-3}$ and a column density $N(\text{CO})= 10^{19} \text{ cm}^{-2}$. We show the “best temperature” fit, for each pointing, which accounts for the measured fluxes (Table 1). The arrows have the same meaning as above.





This figure "fig3.jpg" is available in "jpg" format from:

<http://arxiv.org/ps/astro-ph/9912448v1>